

# Suspensions with small, spherical particles

SA104X Degree Project in Engineering Physics

Samuel Zackrisson<sup>1</sup>

Supervisor: Anna-Karin Tornberg<sup>2</sup>

<sup>1,2</sup>Department for Numerical Analysis, Royal Institute of Technology

<sup>1</sup>samuelz@kth.se

<sup>2</sup>akto@kth.se

May 3, 2015

Analytic solutions for systems of many particles in fluid dynamics and electrostatics are few and far-between. Simulations are therefore essential to studying these systems. This is commonly done without directly calculating the fluid's velocity field. Calculating the field in a three dimensional setting on a cubic grid is  $O(N^3)$ , so finding efficient and accurate methods are of great interest. In this report a method using the spectral accuracy of the fourier transform is studied. The method is applied to a ball of particles sedimenting in a fluid affected by gravity. The properties of this method are compared to similar studies of the same system. The purpose is to map and evaluate the properties this method in comparison with present work.

## Contents

<b>1</b>	<b>Introduction</b>	<b>2</b>
1.1	Sedimenting suspensions of small particles . . . . .	2
1.2	Purpose of this study . . . . .	3
1.3	Delimitations . . . . .	3
<b>2</b>	<b>Theory</b>	<b>3</b>
2.1	Stokes flow . . . . .	3
2.2	Fourier analysis . . . . .	4
2.3	Discretization . . . . .	5
2.4	Regularization . . . . .	5
2.4.1	Triangle functions . . . . .	6

2.4.2	Cardinal splines . . . . .	7
2.5	Other simulation methods . . . . .	8
<b>3</b>	<b>Setup and algorithms</b>	<b>9</b>
3.1	The scene . . . . .	9
3.2	The four-step simulation . . . . .	9
3.3	The particle cloud setup used here . . . . .	10
<b>4</b>	<b>Results</b>	<b>10</b>
4.1	Verifying some fundamental properties of the methods . . . . .	10
4.1.1	Convergence of the Stokes flow . . . . .	10
4.1.2	Characteristics of solutions for regularized singular forcing functions	11
4.1.3	Convergence for regularization scaling with the grid . . . . .	12
4.1.4	Fourier Convergence results . . . . .	12
4.2	Comparing the solutions with other known methods . . . . .	12
4.2.1	Scaling the primitive periodic cell . . . . .	13
4.3	Macroscopic phenomena . . . . .	13
<b>5</b>	<b>Discussion</b>	<b>14</b>
<b>6</b>	<b>Conclusions</b>	<b>14</b>
<b>7</b>	<b>Appendices</b>	<b>15</b>
7.1	Appendix A: Assuming periodicity . . . . .	15

## 1 Introduction

### 1.1 Sedimenting suspensions of small particles

Analytic solutions for systems of many particles in fluid dynamics and electrostatics are few and far-between. Simulations are therefore essential to studying these systems. This is commonly done without directly calculating the fluid's velocity field as in as in a three dimensional setting with  $N$  gridpoints along each dimension gives an  $O(N^3)$  scale to the problem [4]. Finding fast methods of performing calculations on this large set can be simplified by making the perhaps controversial assumption of a periodic grid - assuming that the  $N^3$ -point cube is replicated much like the primitive cells of a crystal lattice. This introduces a periodicity which makes room for fourier methods and - for smooth functions - spectral (exponential) convergence in solutions and the use of the fast fourier transform, which in some places reduced the complexity to  $O(N \log N)$  [5]. In this project a specific method of using the fourier transform is studied, applied to a ball of particles sedimenting in a fluid affected by gravity, and compared to similiar studies of the same system. The purpose is to evaluate this method in comparison with present work on the same simulation.

## 1.2 Purpose of this study

To implement a spectral method for simulation of small, spherical particles sedimenting in a fluid.

To verify some fundamental properties of the methods used.

To compare this method to other methods employed by others. This is done by looking at convergence, differences in flow etc.

To compare how this method introduces new and preserves macroscopic phenomena, compared to how the other methods behave.

## 1.3 Delimitations

We confine ourselves to microhydrodynamics.  $Re \ll 1$ .

I limit the point2grid interp to epsilon hats and delta blobs.

I limit the grid2point interp to some simple built-in function.

I limit the time step to Euler forward.

I limit the primitive periodic cell to a cubic  $N \times N \times N$  grid.

I do not go much into comparing the evolution of the point clouds.

## 2 Theory

### 2.1 Stokes flow

For the small particles in an incompressible, viscous fluid in this study, the Reynolds number is assumed to be small ( $Re \ll 1$ ). The general Navier-Stokes equations can under these conditions be approximated as a linear set of equations, the steady Stokes equations. A solution to these equations is called as a *Stokes flow*. For more details on the equations as they appear here, see [2].

The continuity equation for an incompressible fluid appears as

$$\nabla \cdot \mathbf{u} = 0 \tag{1}$$

and the equations for conservation of momentum are

$$\mu \nabla^2 \mathbf{u} = \nabla p - \mathbf{f} \tag{2}$$

Here  $\mu$  is the dynamic viscosity of the fluid,  $\mathbf{u}$  is the velocity field of the fluid,  $p$  is the absolute pressure and  $\mathbf{f}$  is the volume force on the fluid, the *forcing function*.  $\mathbf{u}$ ,  $p$  and  $\mathbf{f}$  are multivariate functions on  $\mathbf{R}^3$ .

The particle system is assumed to be periodic in three dimensions, i.e. the system and all its characteristics within the volume  $[0, L]^3$  is assumed to repeat in the  $x$ -,  $y$ - and  $z$ -directions. In terms of  $\mathbf{f}$ ,

$$\mathbf{f}(\mathbf{r}) = \mathbf{f}(\mathbf{r} + L\mathbf{m}), \quad \forall \mathbf{m} \in \mathbb{Z}^3 \quad (3)$$

Thus if  $\mathbf{f}$  is known in  $[0, L]^3$ , it is known in  $\mathbf{R}^3$ . Analogously  $\mathbf{u}$  and  $p$  are assumed to be periodic.

## 2.2 Fourier analysis

Studying the Stokes equations (1) and (2) in fourier space one can find an explicit solution for  $\mathbf{u}$  in Stokes equations in terms of  $\mathbf{f}$ .

The Fourier series coefficient  $\mathcal{F}(f)_{\mathbf{k}}$  with wavevector  $\mathbf{k}$  of a function  $f$  on the volume  $V = [0, L]^3$  is taken to be

$$\mathcal{F}(f)_{\mathbf{k}} = \int_V f(\mathbf{x}) e^{-\frac{2\pi}{L}i(\mathbf{k} \cdot \mathbf{x})} d\mathbf{x} \quad (4)$$

The coefficients for the gradient coefficients are thus

$$\mathcal{F}(\nabla f)_{\mathbf{k}} = \frac{2\pi}{L} i \mathbf{k} \mathcal{F}(f)_{\mathbf{k}} \quad (5)$$

Taking the fourier transform of (1) and (2) yields a new set of equations,

$$\mathbf{k} \cdot \mathcal{F}(\mathbf{u})_{\mathbf{k}} = 0 \quad (6)$$

$$-\mu \left( \frac{2\pi}{L} \right)^2 |\mathbf{k}|^2 \mathcal{F}(\mathbf{u})_{\mathbf{k}} = i \frac{2\pi}{L} \mathbf{k} \mathcal{F}(p)_{\mathbf{k}} - \mathcal{F}(\mathbf{f})_{\mathbf{k}} \quad (7)$$

By taking the dot product of (7) and using (6) to eliminate  $\mathcal{F}(\mathbf{u})_{\mathbf{k}}$ , a solution for  $\mathcal{F}(p)_{\mathbf{k}}$  is found. Substituting  $\mathcal{F}(p)_{\mathbf{k}}$  in (7) yields a solution for  $\mathcal{F}(\mathbf{u})_{\mathbf{k}}$ ,  $\mathbf{k} \neq \mathbf{0}$ , in terms of  $\mathcal{F}(\mathbf{f})_{\mathbf{k}}$ . Finding  $\mathbf{u}$  is then a matter of applying the inverse fourier transform.

$$\begin{aligned} \mathcal{F}(p)_{\mathbf{k}} &= -i \frac{\mathbf{k} \cdot \mathcal{F}(\mathbf{f})_{\mathbf{k}}}{|\mathbf{k}|^2 2\pi/L} \\ \mathcal{F}(\mathbf{u})_{\mathbf{k}} &= \frac{1}{\mu |\mathbf{k}|^2} \left( \frac{2\pi}{L} \right)^2 \left( \mathcal{F}(\mathbf{f})_{\mathbf{k}} - \mathbf{k} \frac{\mathbf{k} \cdot \mathcal{F}(\mathbf{f})_{\mathbf{k}}}{|\mathbf{k}|^2} \right) \end{aligned} \quad (8)$$

and  $\mathcal{F}(\mathbf{u})_{\mathbf{0}} := 0$ . This can be expressed in real space as

$$\int_V \mathbf{u}(\mathbf{x}) d\mathbf{x} = 0 \quad (9)$$

In physical terms: there is no net flow over the boundaries of the box.

### 2.3 Discretization

The velocity field  $\mathbf{u}$  in  $[0, L]^3$  is represented by a set of values  $\mathbf{u}_{\mathbf{m}} := \mathbf{u}(h(\mathbf{m} - \mathbf{1}))$ , for  $\mathbf{m} \in I = \{(i, j, k) | i, j, k = 1, 2, \dots, N\}$ ,  $h = L/N$  and  $\mathbf{1} = (1, 1, 1)$ . In other words the field  $\mathbf{u}$  is described on a cubic  $N \times N \times N$ -grid by  $\mathbf{u}_{\mathbf{m}}$ ,  $\mathbf{m} \in I$ . The forcing function is analogously represented by the values  $\mathbf{f}_{\mathbf{m}}$ ,  $\mathbf{m} \in I$ . The Stokes flow is calculated directly from  $\mathbf{f}_{\mathbf{m}}$  in (8) using the fast fourier transform in Matlab. The 3D discrete fourier transform  $\hat{f}_{\mathbf{k}}$ ,  $\mathbf{k} \in I$  of a function representation  $\mathbf{f}_{\mathbf{m}}$ ,  $\mathbf{m} \in I$  is given by

$$\hat{f}_{\mathbf{k}} = \sum_{\mathbf{m} \in I} f_{\mathbf{m}} e^{-i \frac{2\pi}{N} \mathbf{k} \cdot (\mathbf{m} - \mathbf{1})}$$

The continuous fourier transform (4) can be approximated using the discrete fourier transform,

$$\begin{aligned} \mathcal{F}(f) &= \int_V f(\mathbf{x}) e^{-\frac{2\pi}{L} i(\mathbf{k} \cdot \mathbf{x})} d\mathbf{x} \\ &\approx \sum_{\mathbf{m} \in I} f_{\mathbf{m}} e^{-i \frac{2\pi}{L} \mathbf{k} \cdot h(\mathbf{m} - \mathbf{1})} h^3 \\ &= h^3 \cdot \hat{f}_{\mathbf{k}} \end{aligned}$$

Given  $\mathbf{f}_{\mathbf{m}}$  the discretized velocity field  $\mathbf{u}_{\mathbf{m}}$  can be calculated from (8) with the fast fourier transform. As the fast fourier transform has spectral convergence in  $N$  the limiting factor for the convergence of solutions is the smoothness of the input, the forcing function  $\mathbf{f}$ .

### 2.4 Regularization

The only contribution to the forcing function in this study is the force of gravity on the system of  $M$  particles,

$$\begin{aligned} \mathbf{f}(\mathbf{x}) &= -\rho g \hat{\mathbf{z}} \sum_{i=1}^M \delta(\mathbf{x} - \mathbf{x}_i) \\ &= -\rho g \hat{\mathbf{z}} \sum_{i=1}^M \delta^r(\mathbf{x} - \mathbf{x}_i) \end{aligned} \tag{10}$$

where  $\rho$  is the relative density of the fluid and the particles,  $g$  is the gravitational constant and  $\hat{\mathbf{z}} = (0, 0, 1)$ .  $\mathbf{x}_i$  is the position of particle  $i$ ,  $i = 1, 2, \dots, M$ . To evaluate the singular function in (10) on the grid an interpolating function  $\delta^r$  is introduced in place of  $\delta$ . This process is called *regularisation*. Two conditions are imposed on this regularisation function:

1.  $\sum_{\mathbf{m} \in \mathbb{Z}^3} h^3 \delta^r(h\mathbf{m} - \mathbf{x}_0) = 1$  for all  $\mathbf{x}_0$ . This is a discrete version of  $\int \delta(\mathbf{x}) d\mathbf{x} = 1$ .
2.  $\delta^r$  should be as smooth as possible. The smoothness determines the convergence of solutions to (8).

3.  $\delta^r$  should have a small, compact support. This allows for relatively cheap calculation of the forcing function in real space.

Two such choices of functions are discussed in this report, mainly based on the methods in [3] and [6]. These choices for  $\delta^r$  are constructed from univariate functions,  $\delta^r(\mathbf{x}) = \delta_1^r(x)\delta_1^r(y)\delta_1^r(z)$ .

#### 2.4.1 Triangle functions

Perhaps the simplest choice of  $\delta_1^r$  is

$$\delta_1^r(x) = \frac{1}{\epsilon} \max\left(1 - \frac{|x|}{\epsilon}, 0\right) \quad (11)$$

for some small  $\epsilon$ . For  $\epsilon = ph$ ,  $p \in \mathbb{Z}^+$ , this choice of  $\delta^r$  does indeed satisfy the first condition.

$$\sum_{\mathbf{m} \in \mathbb{Z}^3} h^3 \delta^r(h\mathbf{m} - \mathbf{x}_0) = \sum_{i \in \mathbb{Z}} \sum_{j \in \mathbb{Z}} \sum_{k \in \mathbb{Z}} h \delta_1^r(hi - x_0) h \delta_1^r(hj - y_0) h \delta_1^r(hk - z_0) \quad (12)$$

which by translation symmetry is equal to the cube of

$$\begin{aligned} \sum_{i \in \mathbb{Z}} h \delta_1^r(hi - x_0) &= \sum_{i \in \mathbb{Z}} h \cdot \frac{1}{\epsilon} \max\left(1 - \frac{|hi - x_0|}{\epsilon}, 0\right) \\ &\quad \{wlog \ x_0 \in [0, h)\} \\ &= \frac{h}{\epsilon} \sum_{i=-(p-1)}^p 1 - \frac{|hi - x_0|}{\epsilon} \\ &= \frac{2hp}{\epsilon} - \sum_{i=1}^p \frac{hi - x_0}{\epsilon^2} - \sum_{i=-(p-1)}^0 \frac{x_0 - hi}{\epsilon^2} \\ &= \frac{2hp}{\epsilon} - \frac{2h}{\epsilon^2} \left(2\frac{p(p+1)}{2} - p\right) \\ &\quad \{hp = \epsilon\} \\ &= 1 \end{aligned}$$

The function is continuous but without a continuous derivative. Therefore the fourier coefficients of  $\delta^r$  decrease as  $k^{-1}$ .

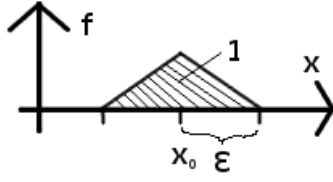


Figure 1: Qualitative image of the triangle function choice of  $\delta^r$ .

### 2.4.2 Cardinal splines

Another choice of  $\delta_1^r$  is found by using the cardinal B-splines  $M_p$  of integer order  $p$ ,  $p \geq 2$  described in [1] and [3] and displayed in figure 2,

$$M_p(u) = \frac{1}{(p-1)!} \sum_{j=0}^p (-1)^j \frac{p!}{j!(p-j)!} (u-j)_+^{p-1} \quad (13)$$

where  $(x)_+ := \max(x, 0)$ .  $M_p$  is nonzero on  $(0, p)$  and is shown in [1] to satisfy the following recursive relations with  $M_2(u) = (1 - |u - 1|)_+$ ,

$$M_p(u) = \frac{u}{p-1} M_{p-1}(u) + \frac{p-u}{p-1} M_{p-1}(u-1) \quad (14)$$

$$\frac{d}{du} M_p(u) = M_{p-1}(u) - M_{p-1}(u-1) \quad (15)$$

The regularisation function is

$$\delta_1^r(hi - x_0) = h^{-1} \cdot M_p(h^{-1}(hi - x_0) + \frac{p}{2})$$

where the term  $\frac{p}{2}$  translates the function graph to be symmetric around  $hi = x_0$ . This function is nonzero for  $|hi - x_0| \leq \frac{ph}{2} \Leftrightarrow i \in (\frac{x_0}{h} - \frac{p}{2}, \frac{x_0}{h} + \frac{p}{2})$ . The resulting  $\delta^r$  satisfies the first condition. It splits into a cube as in (12), and

$$\begin{aligned} \sum_{i \in \mathbb{Z}} h \delta_1^r(hi - x_0) &= \sum_{i \in \mathbb{Z}} h \cdot h^{-1} \cdot M_p(h^{-1}(hi - x_0) + \frac{p}{2}) \\ &= \sum_{i=0}^p M_p(i + \xi) \end{aligned} \quad (16)$$

for some  $\xi \in [0, 1)$  because of translation symmetry and the compact support  $[0, p]$  of  $M_p$ .  $\sum_{i=\xi}^p p + \xi$  is taken to mean that  $i$  is taken in increments of 1. By using the recursion in (14) the expression in (16) can be shown to be 1 by induction.  $M_2$  is in fact a triangle

function from section 2.4.1 and has already been proven to sum to 1. Assuming (16) equals 1 for  $p - 1$  and any  $\xi$ ,

$$\begin{aligned}
\sum_{i=\xi}^{p+\xi} M_p(i) &= \frac{1}{p-1} \sum_{i=\xi}^{p+\xi} i M_{p-1}(i) + (p-i) M_{p-1}(i-1) \\
&= \sum_{i_1=\xi}^{p+\xi} M_{p-1}(i_1-1) + \frac{1}{p-1} \sum_{i_2=\xi}^{p+\xi} i_2 M_{p-1}(i_2) - \frac{1}{p-1} \sum_{i_3=\xi}^{p+\xi} (i_3-1) M_{p-1}(i_3-1) \\
&= \{j_1 = i_1 - 1, j_2 = i_2, j_3 = i_3 - 1\} \\
&= \sum_{j_1=\xi}^{(p-1)+\xi} M_{p-1}(j_1) + 0 + \frac{1}{p-1} \sum_{j_2=\xi}^{p+\xi} j_2 M_{p-1}(j_2) + 0 - \sum_{j_3=\xi}^{p+\xi} j_3 M_{p-1}(j_3) - 0 \\
&= 1
\end{aligned}$$

As  $M_2$  is continuous it is easily deduced from (15) that  $M_p$  is continuously differentiable  $p - 2$  times.

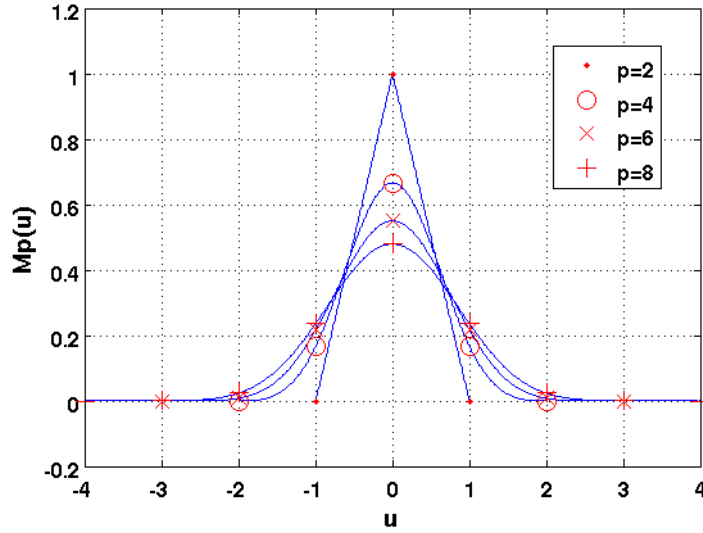


Figure 2: Comparison of the first four even orders of cardinal B-splines, translated to be symmetric in the origin.

## 2.5 Other simulation methods

To circumvent the problem of calculating the Stokes flow in the simulated region a method based on the Greens function can be used. The solution to the Stokes equations in (2)



in  $\mathbb{R}^3$  for the choice  $\mathbf{f}(\mathbf{x}) = \delta(\mathbf{x})$  is the Stokeslet,

$$[Stokeslet] \tag{17}$$

which gives a solution for  $\mathbf{u}$  in (10),

$$[Solutionsum] \tag{18}$$

...and maybe some mention of Ewald summation or similar.

### 3 Setup and algorithms

#### 3.1 The scene

The system in question is a cloud of  $M$  particles randomly placed within a sphere of radius  $r_0$ . This sphere begins in the center of a primitive cell, a cube of side length  $L$ , which is periodically repeated throughout space.

The particles are affected by a gravitational force downward and a lift from the fluid. The resulting force on the particles is the sole driving force in the simulation.

The force from the particles on the fluid make up the forcing function in Stokes' equation.

#### 3.2 The four-step simulation

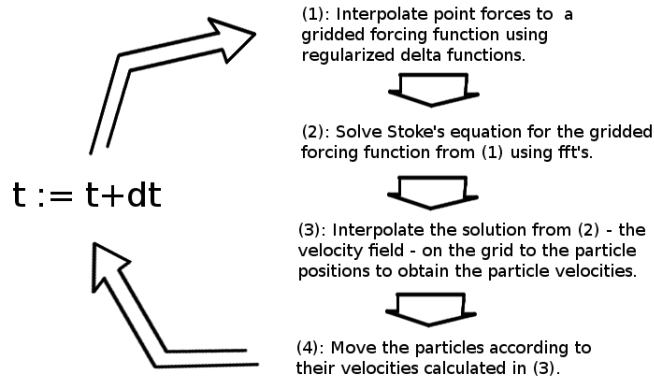


Figure 3: The simulation algorithm steps

Each timestep the simulation has four distinct moments, as illustrated in figure 3.

1. Interpolating from particle positions to grid positions  
 The gravitational force on the particles manifests as singular functions in the Stokes' equation forcing function. To evaluate this force on the grid, the singular functions are regularized to the grid by representing them with regularized  $\delta$ -functions and evaluating these on the grid.  
 This interpolates the  $M$  point forces to a forcing function on the  $N^3$ -grid.
2. Solving Stokes' equation  
 Given the forcing function it is a matter of solving Stokes' equation. This is done using the fft (and thereby the periodicity assumption), giving the following formula derived in appendix.
3. Interpolate the velocity field to the particle positions  
 This is simply done by cubic interpolation using Matlab's builtin function *gridinterp*.
4. Timestepping the particles  
 Given the particle velocities, the particles' positions can now be calculated using Euler's method.

If the only interest is studying the velocity field solution on the grid, steps 1-2 are sufficient. This can be done for any time  $t$  in the simulation, as Stokes' equation is *memoryless*, it does not depend on the history of neither the velocity field nor the forcing functions.

### 3.3 The particle cloud setup used here

Two systems of particles are studied in this article. The first and simplest systems has  $M = 3$  particles placed along a central  $z$ -axis in the primitive cell, two clustered to display the increase in velocity as they drag more fluid together. The second, larger system has a cloud of  $M 10^3$  particles uniformly distributed over a ball, initially in the center of the primitive cell. This is similar to the system studied in [4].

## 4 Results

### 4.1 Verifying some fundamental properties of the methods

#### 4.1.1 Convergence of the Stokes flow

The convergence of the solution obtained through (8) depends on the smoothness of the forcing function  $\mathbf{f}$ . The convergence of solutions for a smooth and a non-smooth forcing function can be seen in figure 4. The smooth function is ( $L = 2.0$ )  $g_1(x, y, z) = \sin(L \cos(\frac{2\pi}{L}x)) \cos(\frac{2\pi}{L}y) + \sin(\frac{2\pi}{L}z)$  and the non-smooth is  $g_2(x, y, z) = \sin(\frac{2\pi}{L}x) \cos(\frac{2\pi}{L}y) (\frac{2}{L^2}z^3 -$

$\frac{3}{L}z^2 + z$ ).  $g_2$  is continuously differentiable once. The non-smooth solution converges as  $N^{-2.29}$ .

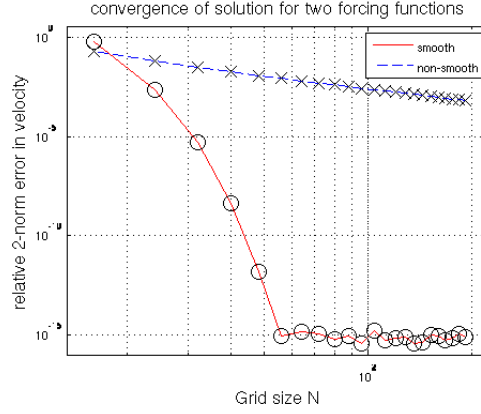


Figure 4: Comparison of the Stokes flow solutions for a smooth and a non-smooth forcing function.

#### 4.1.2 Characteristics of solutions for regularized singular forcing functions

Here the forcing function in (10) is introduced. The regularized forcing functions and respective solutions to Stokes equations for a system with  $M = 3$  particles along a central line along the  $z$ -axis is displayed in figure 5

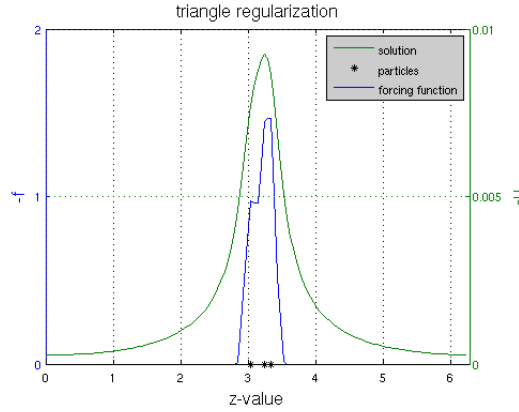


Figure 5: The particle positions, shape of the regularized point forces and Stokes flow for given particle positions. Here  $L = 2\pi$ ,  $N = 128$ ,  $\epsilon = 4h$ .

#### 4.1.3 Convergence for regularization scaling with the grid

#### 4.1.4 Fourier Convergence results

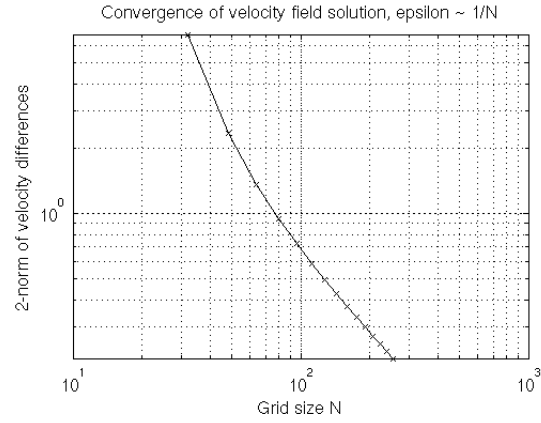


Figure 6: Normed successive differences in solutions as N increases and epsilon decreasing with it.

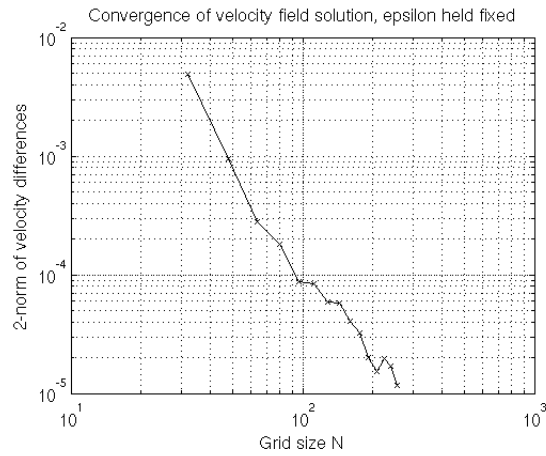


Figure 7: Normed successive differences in solutions as N increases, keeping epsilon fixed.

## 4.2 Comparing the solutions with other known methods

The system studied in this article is not the same system initially presented. The system uses discretized functions and an assumption of periodicity has been made. It is thus

of interest to study how this simulation method compares to other takes on the particle system.

#### 4.2.1 Scaling the primitive periodic cell

If the cloud of particles is of the same magnitude as the period of the system it is not unlikely to have interactions between clouds of different primitive cells. This can be studied by scaling the length of the primitive cells while keeping the particle cloud size fixed and looking at the differences between successive solutions for the velocity field in a cube of fixed size containing the particle cloud. For simple triangle functions, the successive relative differences decrease as  $L^{-1.30}$ . However, the meaning of this measure is not entirely obvious. For each value of  $L$  a different physical system is studied. The solutions for these systems should converge to the non-periodic case as  $L \rightarrow \infty$ .

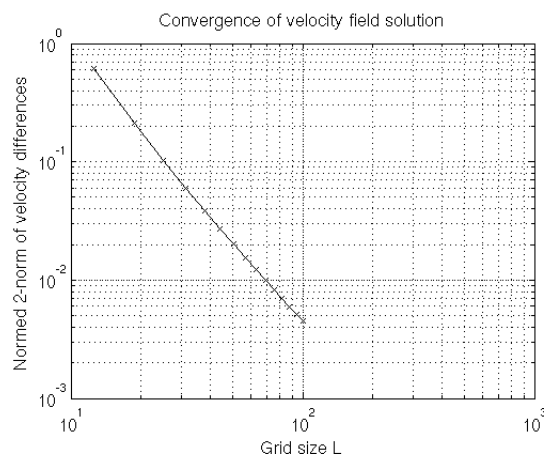


Figure 8: Normed successive differences in solutions as the primitive cell increases.

#### 4.3 Macroscopic phenomena

The evolution of the cloud shape in a periodic box appears to agree with that observed by Metzger et al [4] in a non-periodic setting. The sedimenting ball becomes oblate, forms a torus (see Figure 9) and eventually breaks into two smaller clouds. This can be compared in more detail by studying e.g. the particle density along the z-axis in the cloud center, the pressure gradient in and surrounding the cloud, the velocity field in and around the cloud.

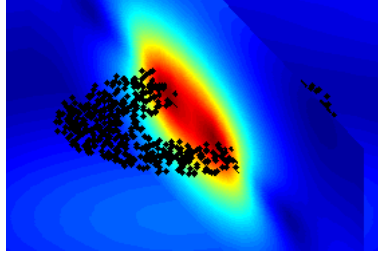


Figure 9: The torus shape the cloud evolves into [plot missing axes, units, #steps,  $dt=0.01$ ,  $N=32$ ,  $M=1000$  etc]

For too few gridpoints the cloud appears to take a square shape aligned with the grid cells, see Figure 10. When this effect in practice disappears can be studied further, e.g. by plotting the particle density as a function of azimuthal angle.

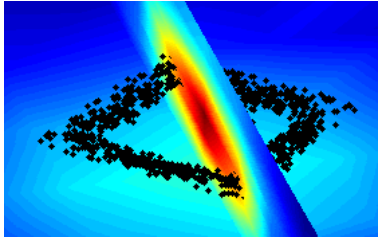


Figure 10: The square shape of the torus cloud for  $N=8$  [plot missing axes, units, #steps,  $dt=0.001$ ,  $N=8$ ,  $M=1000$  etc]

## 5 Discussion

## 6 Conclusions

## References

- [1] Ulrich Essmann, Lalith Perera, Max L. Berkowitz, Tom Darden, Hsing Lee, and Lee G. Pedersen. A smooth particle mesh ewald method. *The Journal of Chemical Physics*, 103:8577–8593, 1995.
- [2] Élizabéth Guazzelli and Jeffrey F. Morris. *A Physical Introduction to Suspension Dynamics*. Cambridge University Press, 1 edition, 2012.
- [3] Dag Lindbo and Anna-Karin Tornberg. Spectral accuracy in fast ewald-based methods for particle simulations. *Journal of Computational Physics*, 230:8744–8761, 2011.

- [4] Bloen Metzger, Maxime Nicolas, and Élizabeth Guazzelli. Falling clouds of particles in viscous fluids. *J. Fluid Mech.*, 580:283–301, 2007.
- [5] David Saintillan, Eric S.G. Shaqfeh, and Eric Darve. The growth of concentration fluctuations in dilute dispersions of orientable and deformable particles under sedimentation. *J. Fluid Mech.*, 553:347–388, 2006.
- [6] Anna-Karin Tornberg and Björn Engquist. Numerical approximations of singular source terms in differential equations. *Journal of Computational Physics*, 200:462–488, 2004.

## **7 Appendices**

### **7.1 Appendix A: Assuming periodicity**